

Power requirement of the geodynamo from ohmic losses in numerical and laboratory dynamos

Ulrich R. Christensen¹ & Andreas Tilgner²

¹Max-Planck-Institut für Aeronomie, Max-Planck-Strasse 2, 37191 Katlenburg-Lindau, Germany

²Institut für Geophysik, Universität Göttingen, Herzberger Landstrasse 180, 37075 Göttingen, Germany

In the Earth's fluid outer core, a dynamo process converts thermal and gravitational energy into magnetic energy. The power needed to sustain the geomagnetic field is set by the ohmic losses (dissipation due to electrical resistance)¹. Recent estimates of ohmic losses cover a wide range, from 0.1 to 3.5 TW, or roughly 0.3–10% of the Earth's surface heat flow^{1–4}. The energy requirement of the dynamo puts constraints on the thermal budget and evolution of the core through Earth's history^{1–5}. Here we use a set of numerical dynamo models to derive scaling relations between the core's characteristic dissipation time and the core's magnetic and hydrodynamic Reynolds numbers—dimensionless numbers that measure the ratio of advective transport to magnetic and viscous diffusion, respectively. The ohmic dissipation of the Karlsruhe dynamo experiment⁶ supports a simple dependence on the magnetic Reynolds number alone, indicating that flow turbulence in the experiment and in the Earth's core has little influence on its characteristic dissipation time. We use these results to predict moderate ohmic dissipation in the range of 0.2–0.5 TW, which removes the need for strong radioactive heating in the core⁷ and allows the age of the solid inner core to exceed 2.5 billion years.

The limited thermodynamic efficiency of thermal convection means that the power available to drive the dynamo is only a fraction of the total heat flow from the core. Compositional convection, driven by the rejection of light alloying elements from the growing solid inner core, is not limited by Carnot efficiency, but is intimately associated with core cooling. The heat flow from the core must be 5–10 times larger than the ohmic dissipation¹. For high dissipation, the core has to supply a substantial part of the Earth's heat. If this heat flow is due to secular cooling alone, as is conventionally assumed, it implies unrealistic core temperatures early in Earth's history^{1,3}. Significant radiogenic heat production in the core (for example, from decay of ⁴⁰K) would be needed to avoid this. If the core cools rapidly, the solid inner core would have formed only 1 Gyr ago³. It is clearly important to better constrain the actual power requirements of the dynamo.

The observed geomagnetic field could be maintained, in principle, by currents that produce <1 GW of ohmic dissipation², but the actual losses are believed to be much larger. Ohmic dissipation is given by

$$D_{\text{ohm}} = \int (\eta/\mu_0)(\nabla \times \mathbf{B})^2 dV \propto 2\eta E_{\text{mag}}/l_B^2 \quad (1)$$

where η is magnetic diffusivity, μ_0 magnetic permeability, \mathbf{B} magnetic field, E_{mag} magnetic energy and l_B the characteristic length scale of the field. Estimating the ohmic dissipation of the geodynamo suffers from several sources of uncertainty—for example, the magnetic field strength inside the core. More importantly, the scale of the core field is unknown, because magnetization of the Earth's crust shields wavelengths below 3,000 km from observation⁸. Recent geodynamo models can reproduce basic properties of the geomagnetic field, and have been used to estimate ohmic dissipation^{1,2,9,10}. However, the values of some model

parameters are far from Earth-like. In particular, the Ekman number $E = \nu/(\Omega R^2)$, measuring viscous forces relative to rotational forces, and the magnetic Prandtl number $\text{Pm} = \nu/\eta$, are far too large (ν is viscosity, Ω rotation frequency and R core radius). Several models use hyperdiffusivities that suppress small scales in the magnetic and flow fields. A rather low ohmic dissipation of about 0.1–0.3 TW has been estimated when small-scale contributions are ignored^{1,2}. An extrapolation to account for these scales, using the magnetic power spectrum at the core–mantle boundary from a high-resolution dynamo model¹⁰, predicted 1–2 TW of total ohmic dissipation².

Rather than using a single dynamo, we determine the time-average ohmic dissipation in a suite of 24 models, varying the key non-dimensional numbers by factors of 20–30. This allows us to study systematically the dependence on the control parameters and to derive scaling laws that are applicable to the geodynamo. Because the magnetic energy differs substantially between models, we do not

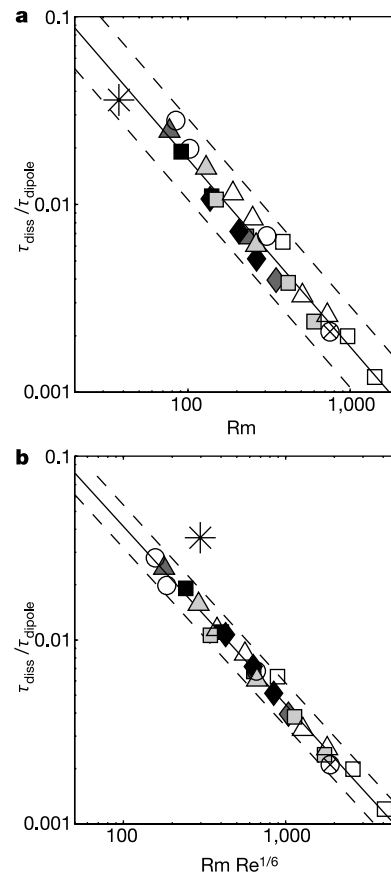


Figure 1 Scaling of magnetic dissipation time. **a**, **b**, Dissipation time in units of dipole decay time versus magnetic Reynolds number (**a**) and versus a combination of magnetic and hydrodynamic Reynolds numbers (**b**). The magnetic Prandtl number is 2–3 for open symbols, 1 for light grey, 0.5 for dark grey and 0.15–0.25 for black symbols. The Ekman numbers are 1.27×10^{-4} (circles), 4.2×10^{-5} (triangles), 1.27×10^{-5} (squares) and 4.2×10^{-6} (diamonds). The reversing dynamo is marked by a circled cross. Best-fitting lines with a slope of -1.0 in **a** and -0.97 in **b** and 3σ limits (broken lines) are drawn. The mean misfit is 16% in **a** and 9% in **b**. All dynamos have been run for at least 40 advection times (R/U), and averages have been taken after the transient adjustment. The numerical resolution varies between 53 and 168 in spherical harmonic degree and 33 and 81 radial points, depending on parameters. At the lowest Ekman number, twofold symmetry in longitude has been assumed; all other cases are for a full sphere. The large asterisk is for the Karlsruhe laboratory dynamo. For the laboratory dynamo the magnetic Reynolds number is based on the cylinder radius R , whereas the hydrodynamic Reynolds number is calculated with the width of the flow ducts $d = 0.05$ m.

scale D_{ohm} directly, but rather scale the magnetic dissipation time:

$$\tau_{\text{diss}} = E_{\text{mag}}/D_{\text{ohm}} \propto I_B^2/2\eta \quad (2)$$

For our models we solve the full magnetohydrodynamic equations without hyperdiffusivities for an incompressible fluid in a rotating spherical shell¹¹. The magnetic fields are dipole-dominated, mostly with stable polarity. We include one case with dipole reversals similar to those in the geomagnetic field¹².

A large-scale magnetic field is converted by nonlinear interaction with the flow field to small scales where it is dissipated. The important parameter for this process is the magnetic Reynolds number $Rm = UR/\eta$, with the r.m.s. velocity U . In Fig. 1a we plot magnetic dissipation time versus Rm and find a simple fit of the form:

$$\tau_{\text{diss}}/\tau_{\text{dipole}} = 1.74 Rm^{-1} \quad (3)$$

Here we normalize with the dipole decay time, $\tau_{\text{dipole}} = R^2/(\pi^2\eta)$, for a full sphere, which is the longest possible time constant for decay of a magnetic field in a stagnant conductor. Cases with lower magnetic Prandtl number (darker shading in Fig. 1a) tend to plot below the fitting line, and those with higher Pm tend to fall above the line. This suggests an additional dependence on Pm , or expressed differently, on the hydrodynamic Reynolds number $Re = Rm/Pm$. A best fit of the form:

$$\tau_{\text{diss}}/\tau_{\text{dipole}} = a(Rm Re^b)^c \quad (4)$$

with $a = 3.58$, $b = 1/6$ and $c = -0.97$, reduces the scatter somewhat (Fig. 1b). We find no clear influence of the Ekman number. The dependence on Re is weak, but to apply equation (4) to the core requires extrapolation over six orders of magnitude in Re , and leads to a factor of ten difference in τ_{diss} compared with equation (3). Adding more free parameters always reduces the misfit, hence one may question if a dependence on Re is really warranted, and if so, whether it also holds for much larger values of the Reynolds number.

In order to resolve this question, we analyse the ohmic dissipation

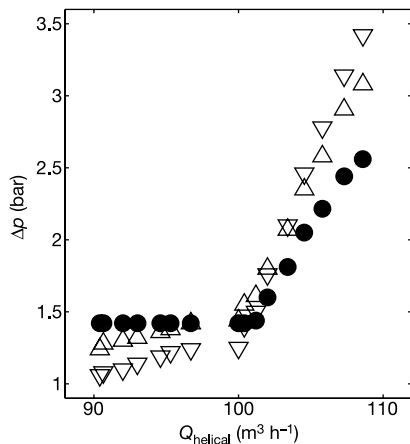


Figure 2 Pressure drop versus flow rate in the Karlsruhe dynamo experiment. Three independent pumps send sodium through disjoint flow loops, two of which are designated as ‘helical’ and one as ‘axial’ because of the shape of the path followed by the flow. The cylinder formed by the pipes has a radius $R = 0.95$ m and similar height. Triangles show the pressure drop Δp in the helical loops, and circles that in the axial loop versus flow rate Q_{helical} in the helical loops. The flow in the axial loop is held constant at $112.5 \text{ m}^3 \text{ h}^{-1}$. Above the onset of dynamo action at $Q_{\text{helical}} \approx 100 \text{ m}^3 \text{ h}^{-1}$, the ohmic dissipation is calculated as $D_{\text{ohm}} = \Sigma Q_i(\Delta p_i - \Delta p_i^v)$, where the summation is over the three loops. The contribution of viscous friction to the pressure drop Δp^v is obtained by extrapolating Δp from below the threshold of dynamo action. We extrapolate (interpolate) the data to a reference state with $Q = 111 \text{ m}^3 \text{ h}^{-1}$ in all three loops, for which the magnetic field was measured inside the cylinder without recording the pressure drop.

of the Karlsruhe laboratory dynamo^{6,13}, where liquid sodium is pumped through a system of pipes arranged into cells forming a nearly homogeneously conducting cylinder. Here the hydrodynamic Reynolds number is 2.5×10^5 , based on the size of the largest possible turbulent eddies, and the magnetic Prandtl number is 9×10^{-6} , whereas in the models $Re < 500$ and $Pm \geq 0.15$. When the flow rate exceeds a threshold, dynamo action sets in and a sharp rise in the driving pressure drop can be used to calculate the ohmic dissipation (Fig. 2). In order to calculate τ_{diss} , the magnetic energy must be known. We obtain this energy by fitting the magnetic field of a dedicated kinematic dynamo simulation to field measurements performed along the cylinder axis and outside the sodium. A simpler version of this model predicted successfully the onset of dynamo action¹⁴. Finally, we normalize τ_{diss} with the numerically calculated dipole decay time $\tau_{\text{dipole}} = 0.79$ s. The result, marked by an asterisk in Fig. 1, agrees well with the simple scaling on the magnetic Reynolds number alone. The additional dependence on the hydrodynamic Reynolds number under-predicts the dissipation time by a factor of 2.5 (Fig. 1b), which is far outside the estimated uncertainty for the experimental value of 40% and the 3σ limit of the fit to the numerical results. A dependence of τ_{diss} on Re might be plausible, because the small eddies that occur in the flow at high Re

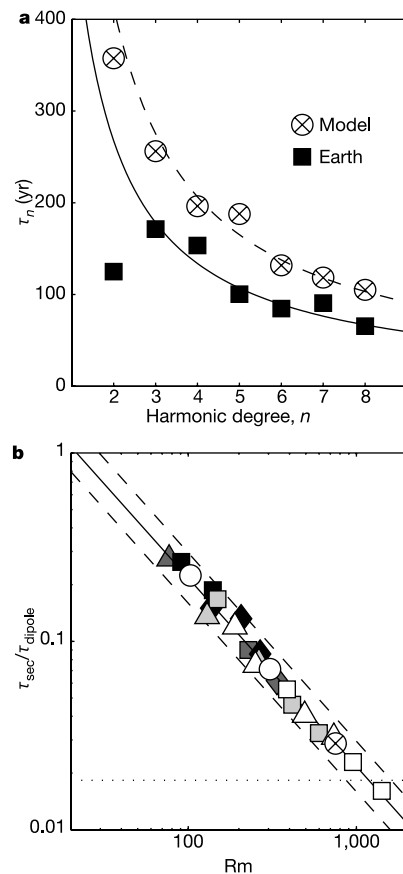


Figure 3 Secular variation time scaling. **a**, Timescale τ_n of secular variation as function of spherical harmonic degree n for the geomagnetic field in the time interval 1840–1990 and, as an example, for the long-term average of the reversing dynamo model. The model data are scaled to real time with $\tau_{\text{dipole}} = 29,000$ yr, obtained for an electrical conductivity $\sigma = \mu_0/\eta = 6 \times 10^5 \text{ S m}^{-1}$ in the core²⁰. Fitting lines of the form $\tau_n = \tau_{\text{sec}}/n$ are included. **b**, Secular variation timescales τ_{sec} of the dynamo models versus magnetic Reynolds number. The fitting line is $\tau_{\text{sec}}/\tau_{\text{dipole}} = 21.7 Rm^{-1}$. The dotted horizontal line indicates the Earth value estimated from the fit in **a**, 535 yr in physical units. The predicted $Rm \approx 1,200$ agrees well with the value obtain from estimates of $U = 12\text{--}15 \text{ km yr}^{-1}$ obtained by inverting geomagnetic secular variations for the fluid flow near the core surface²¹.

(low Pm), together with the large-scale flow, may be more efficient in transporting magnetic energy to small scales. However, such an effect will vanish in any case when the turbulent eddies become smaller than the length scale l_B at which diffusion dissipates magnetic energy. One interpretation of our finding is that a weak dependence on the magnetic Prandtl number at values $Pm \approx 1$ disappears for $Pm < 1$. We therefore suggest that the simpler scaling law (equation (3)) represents Earth's core conditions reasonably well.

In order to calculate the dissipation of the geodynamo, we must know Rm and the total magnetic energy in the core. We use the dependence of the secular variation on Rm in our dynamo models to estimate the core value. The timescale of secular variation depends on the spherical harmonic degree n , and is defined as:

$$\tau_n = \left[\frac{\left\langle \sum_{m=0}^n (g_{nm}^2 + h_{nm}^2) \right\rangle}{\left\langle \sum_{m=0}^n (g_{nm}^2 + h_{nm}^2) \right\rangle} \right]^{1/2}$$

where g, h are the Gauss coefficients, the dot marks their time derivative and $\langle \rangle$ the time average. For the geomagnetic field, τ_n decreases with n (ref. 15). To derive a single time constant of secular variation τ_{sec} we attempt a simple fit of the form $\tau_n = \tau_{sec}/n$, although a somewhat stronger dependence on n might better represent the present rate of secular variation (R. Holme, personal communication). Excluding the dipole part, the fit is fair for $n = 2-8$ in the time period 1840-1990 and gives $\tau_{sec} = 535$ yr (Fig. 3a). The secular variation in the dynamo models, averaged over much longer time, follows more closely a $1/n$ -dependence. τ_{sec} depends on the inverse of the magnetic Reynolds number (Fig. 3b). The estimated secular variation time of the geomagnetic field requires Rm = 1,200 in the core, which leads to a magnetic dissipation time of 42 yr.

The factor between the mean magnetic field strength inside the model shell and that in degrees n up to 12 on the outer boundary is in the range of 2.5-5 in our non-reversing dynamos and 7.5 in the reversing case. With a likely factor of 5-7.5 for the geodynamo and an r.m.s. field strength ($n < 13$) at the core-mantle boundary of 0.39 mT (ref. 16), we infer 2-3 mT for the field in the core, which gives $E_{mag} = (2.8-6.2) \times 10^{20}$ J. From equation (2) the ohmic dissipation is found to be 0.2-0.5 TW.

For the recently preferred high-power-consumption values of the geodynamo of >1 TW (refs 2, 3, 17), the required heating could be supplied by >200 p.p.m. potassium in the core¹⁷. Although recent experiments suggest that such concentrations are possible^{7,18}, our result suggesting a more moderate power requirement relaxes severe constraints on core evolution, and removes the strong need for heat sources in the core. The inner core could be much older than 1 Gyr; thermal modelling¹ predicts an inner core age of 2.4 Gyr for $D_{ohm} = 0.5$ TW and ~ 3.5 Gyr for $D_{ohm} = 0.2$ TW. As the geodynamo must operate differently in the absence of an inner core or may not operate at all, the existence of a magnetic field of roughly present-day strength over the past 3.5 Gyr (ref. 19) is more easily reconciled with an old inner core. □

Received 3 February; accepted 22 March 2004; doi:10.1038/nature02508.

1. Buffett, B. A. Estimates of heat flow in the deep mantle based on the power requirements of the geodynamo. *Geophys. Res. Lett.* **29**, doi:10.1029/2001GL014649 (2002).
2. Roberts, P. H., Jones, C. A. & Calderwood, A. R. in *Earth's Core and Lower Mantle* (eds Jones, C. A., Soward, A. M. & Zhang, K.) 100-129 (Taylor & Francis, London, 2003).
3. Labrosse, S. Thermal and magnetic evolution of the Earth's core. *Phys. Earth Planet. Inter.* **140**, 127-143 (2003).
4. Gubbins, D., Alfé, D., Masters, G., Price, D. & Gillan, M. J. Can the Earth's dynamo run on heat alone? *Geophys. J. Int.* **155**, 609-622 (2003).
5. Nimmo, F., Price, G. D., Brodholt, J. & Gubbins, D. The influence of potassium on core and geodynamo evolution. *Geophys. J. Int.* **156**, 363-376 (2004).
6. Stieglitz, R. & Müller, U. Experimental demonstration of the homogeneous two-scale dynamo. *Phys. Fluids* **13**, 561-564 (2001).
7. Gessmann, C. K. & Wood, B. J. Potassium in the Earth's core? *Earth Planet. Sci. Lett.* **200**, 63-78 (2002).
8. Langel, R. A. & Estes, R. H. A geomagnetic field spectrum. *Geophys. Res. Lett.* **9**, 250-253 (1982).
9. Kuang, W. & Bloxham, J. An Earth-like numerical dynamo model. *Nature* **389**, 371-374 (1997).
10. Roberts, P. H. & Glatzmaier, G. A. A test of the frozen-flux approximation using a new geodynamo model. *Phil. Trans. R. Soc. Lond. A* **358**, 1109-1121 (2000).

11. Christensen, U., Olson, P. & Glatzmaier, G. A. Numerical modeling of the geodynamo: a systematic parameter study. *Geophys. J. Int.* **138**, 393-409 (1999).
12. Kutzner, C. & Christensen, U. R. From stable dipolar to reversing numerical dynamos. *Phys. Earth Planet. Inter.* **131**, 29-45 (2002).
13. Müller, U. & Stieglitz, R. The Karlsruhe dynamo experiment. *Nonlin. Proc. Geophys.* **9**, 165-170 (2002).
14. Tilgner, A. Numerical simulation of the onset of dynamo action in an experimental two-scale dynamo. *Phys. Fluids* **14**, 4092-4094 (2002).
15. Hulot, G. & LeMouél, J. L. A statistical approach to the Earth's main magnetic field. *Phys. Earth Planet. Inter.* **82**, 167-183 (1994).
16. Bloxham, J. & Jackson, A. Time-dependent mapping of the magnetic field at the core-mantle boundary. *J. Geophys. Res.* **97**, 19537-19563 (1992).
17. Buffett, B. A. The thermal state of the Earth's core. *Science* **299**, 1675-1676 (2003).
18. Rama Murthy, V., van Westrenen, W. & Fei, Y. Experimental evidence that potassium is a substantial radioactive heat source in planetary cores. *Nature* **423**, 163-165 (2003).
19. McElhinny, M. W. & Senanayake, W. E. Paleomagnetic evidence for the existence of the geomagnetic field 3.5 Ga ago. *J. Geophys. Res.* **85**, 3523-3528 (1980).
20. Secco, R. A. & Schloessin, H. H. The electrical resistivity of solid and liquid Fe at pressures up to 7 GPa. *J. Geophys. Res.* **94**, 5887-5894 (1989).
21. Bloxham, J., Gubbins, D. & Jackson, A. Geomagnetic secular variations. *Phil. Trans. R. Soc. Lond. A* **329**, 415-502 (1989).

Acknowledgements We thank U. Müller for the permission to use unpublished results from the laboratory dynamo experiment. This work was supported by the priority programme "Geomagnetic secular variations" of the Deutsche Forschungsgemeinschaft.

Competing interests statement The authors declare that they have no competing financial interests.

Correspondence and requests for materials should be addressed to U.R.C. (Christensen@linmpi.mpg.de)

Optimal nitrogen-to-phosphorus stoichiometry of phytoplankton

Christopher A. Klausmeier^{1,2}, Elena Litchman^{2,3}, Tanguy Daufresne¹ & Simon A. Levin¹

¹Department of Ecology and Evolutionary Biology, Princeton University, Princeton, New Jersey 08544, USA

²School of Biology, Georgia Institute of Technology, 310 Ferst Drive, Atlanta, Georgia 30332-0230, USA

³Institute of Marine and Coastal Sciences, Rutgers University, New Brunswick, New Jersey 08901, USA

Redfield noted the similarity between the average nitrogen-to-phosphorus ratio in plankton (N:P = 16 by atoms) and in deep oceanic waters (N:P = 15; refs 1, 2). He argued that this was neither a coincidence, nor the result of the plankton adapting to the oceanic stoichiometry, but rather that phytoplankton adjust the N:P stoichiometry of the ocean to meet their requirements through nitrogen fixation, an idea supported by recent modelling studies^{3,4}. But what determines the N:P requirements of phytoplankton? Here we use a stoichiometrically explicit model of phytoplankton physiology and resource competition to derive from first principles the optimal phytoplankton stoichiometry under diverse ecological scenarios. Competitive equilibrium favours greater allocation to P-poor resource-acquisition machinery and therefore a higher N:P ratio; exponential growth favours greater allocation to P-rich assembly machinery and therefore a lower N:P ratio. P-limited environments favour slightly less allocation to assembly than N-limited or light-limited environments. The model predicts that optimal N:P ratios will vary from 8.2 to 45.0, depending on the ecological conditions. Our results show that the canonical Redfield N:P ratio of 16 is not a universal biochemical optimum, but instead represents an average of species-specific N:P ratios.